12th Spanish Conference on Electron Devices

Salamanca, Spain, 14-16 November 2018

CDE 2018

Hospedería Fonseca • Universidad de Salamanca

Program and Abstracts

http://CDE2018.usal.es/

Physical degradation of Ni/HfO_2/n^+-Si resistive switching devices caused by unipolar cycling effects

J. Muñoz-Gorriz[1], M. C. Acero[2], M. B. Gonzalez[2], E. Miranda[1], J. Suñe[1], F. Campabadal[2]

[1] Departament d'Enginyeria Electrònica, Universitat Autònoma de Barcelona, 08193 Bellaterra, Spain
[2] Institut de Microelectrònica de Barcelona, IMB-CNM, CSIC. Campus UAB, 08193 Bellaterra, Spain.
Tel: (+34) 93 581 35 30, Electronic mail: Jordi.munoz.gorriz@uab.cat

1. Abstract

In this work, the physical degradation of Ni/HfO_2/n^+-Si RRAM devices occurring during negative unipolar resistive switching cycling is analyzed. In most of the cases, a localized defect is generated in the dielectric layer after the forming process. However, due to the electrical stress, in some devices a complete degradation is observed comprising a crater-like structure, being this behavior correlated to a sudden increase of the current in the low resistance state.

2. Introduction

Resistive switching random access memories (RRAMs) are emerging non-volatile memories that rely on a reversible oxide breakdown mechanism known as resistive switching (RS). The device switches between two different resistance values: the high resistance state (HRS) and the low resistance state (LRS). Physically, this corresponds to the formation and rupture of a conductive filament (CF) spanning the dielectric film [1]. The performance and reliability of these devices are currently under extensive investigation because RRAM is a promising candidate to substitute flash technology [2]. In this work, the physical degradation of Ni/HfO_2/n^+-Si devices caused by RS cycling has been analyzed and the impact on the device performance evaluated.

3. Experimental

The investigated devices are field-oxide isolated Ni/HfO_2/n^+-Si capacitors with two HfO_2 thicknesses (20 nm and 10 nm), and two active areas (5×5 μm^2 and 2×2 μm^2) (Fig. 1). The electrical characterization was carried out using a HP-4155B semiconductor parameter analyzer, applying voltage sweeps to the Ni electrode with the Si substrate grounded. As these devices present unipolar RS [3], RS cycling has been performed applying negative voltage sweeps. In Fig. 2 an example of the RS current-voltage (I-V) characterization process is shown. An initial sweep (forming) activates the RS property leading the device to the LRS. Then, the RS cycling is performed by applying negative voltage sweeps: the reset process switches the device from the LRS to the HRS; and the set switches from the HRS to the LRS. In the forming and set processes, the current was limited to 100 µA to avoid irreversible breakdown.

After the electrical measurements, the Ni layer was etched off by means of the solution (H_2O:HNO_3)(4:1) so that the HfO_2 surface was exposed. After this etching process, the dielectric was inspected using a scanning electron microscope (SEM).

4. Results and Discussion

Fig. 3 shows typical SEM images obtained after removing the Ni electrode. In most of the devices inspected, a small hillock is observed (Fig. 3(a)), which is likely located at the CF position [4]. However, in some samples, the entire active area of the device is degraded, showing a crater-like structure (Fig. 3(b)). This aggressive degradation of the device is observed for both dielectric thicknesses but only in devices with the smallest active area (2×2 μm^2). Fig. 4 shows the current-voltage (I-V) characteristics corresponding to the sample shown in Fig. 3(b). Notice that at some RS cycle, the reset process (reset no. 12 in this case) shows a sudden increase of the current above 10 mA. A similar current increase has been observed in all the severely damaged samples. The analysis of the results reveals that, after the current overshoot, $|V_{set}|$ and $|V_{reset}|$ progressively decrease with the cycle number (Fig. 5(a)), while the currents in the LRS (I_{LRS}) and in the HRS (I_{HRS}) measured at a voltage of -0.2 V show a sudden change (Fig. 5(b)). While I_{LRS} increases, I_{HRS} decreases. In addition, the cycle-to-cycle variability is reduced and the memory window is increased. Therefore, in this case the RS characteristics of the device have been improved. After analyzing several samples, it has been concluded that if the current previous to the reset process reaches values higher than 10 mA, due to the thermal processes involved, a physical damage on the device structure is created. This damage has been found to have a considerable impact on the electrical performance.

Acknowledgements

This work has been partially funded by the Spanish Ministry of Science, Innovation and Universities and the FEDER program through projects TEC2017-84321-C4-1-R, TEC2017-84321-C4-4-R, and TEC2014-54906-JIN.

References

[1] J.S. Lee *et al.*, Appl. Phys. Rev., vol. 2, 031303, 2015.
[2] J.S. Meena *et al.*, Nanoscale Res. Lett., vol. 9, 526, 2014.
[3] A. Rodríguez *et al*., Microelectron. Eng., vol. 147, pp. 75-78, 2015.
[4] S. Claramunt *et al.*, Microelectron. Eng., vol. 147, pp. 335-338, 2015.

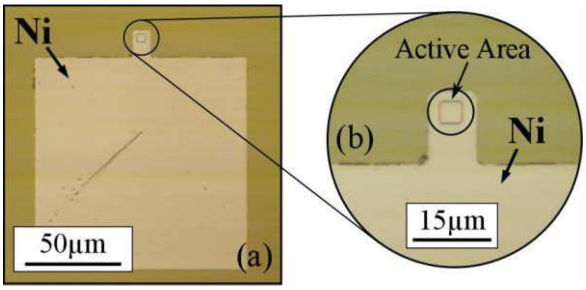

Fig.1. (a) Top-view optical image of a pristine Ni/HfO_2/n^+-Si device. (b) Zoom-in image of the 5×5μm^2 active area.

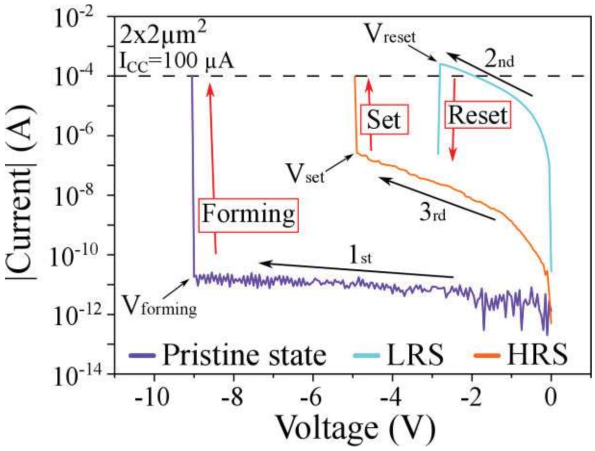

Fig.2. Typical I-V characteristics of a RS cycle performed on a Ni/20nm-HfO_2/n^+-Si sample. The characteristic RS voltages are indicated: forming ($V_{forming}$), set (V_{set}) and reset (V_{reset}) voltages.

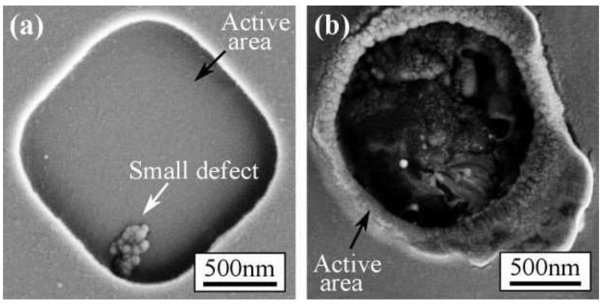

Fig.3. Top-view SEM images after RS cycling and Ni etching of the active area of (a) a standard device, and (b) of the unusually degraded device with the RS characteristics shown in Fig. 4. Both devices have a 10nm thick HfO_2 layer.

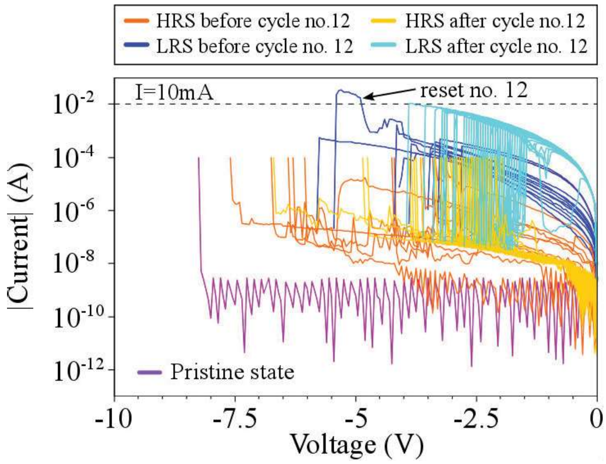

Fig.4. I-V characteristics of a sequence of 100 RS cycles in the Ni/10nm-HfO_2/n^+-Si sample shown in Fig. 3(b).

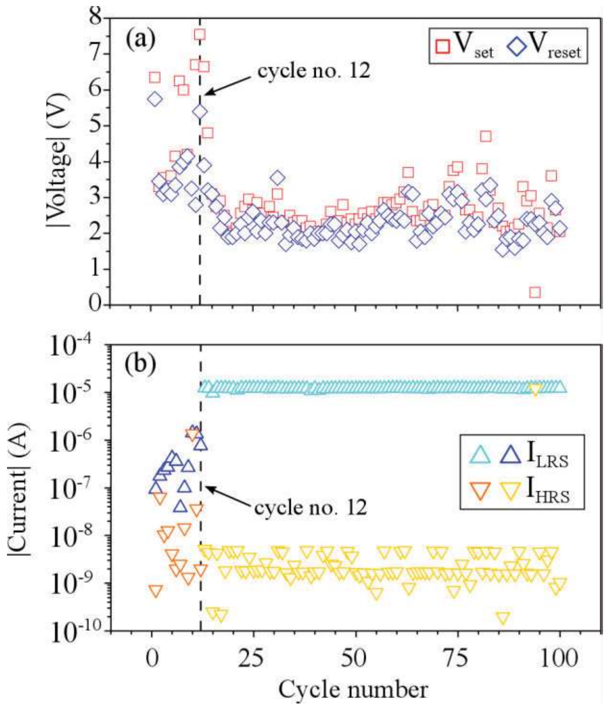

Fig.5. (a) V_{set} and V_{reset} values; and (b) I_{LRS} and I_{HRS} at V=-0.2 V as a function of cycle number, corresponding to the RS cycling characteristics shown in Fig. 4.